IMPROVED FLIGHT CONTROL PERFORMANCE AND FAILURE TOLERANCE USING MODERN CONTROL TECHNIQUES

Howard Berman
Grumman Aerospace Corporation
Bethpage, N.Y., U.S.A.

Abstract

Modern control techniques, including linear optimal control and estimation theory, have been under investigation for many years. However, application to the control of aircraft has been limited. The advent of practical digital flight control systems in recent years gives new impetus to the use of these techniques — particularly with the rapid increase in computational capability of flight-type hardware. This paper outlines an organized computer-aided procedure using modern control techniques to design digital Fly-By-Wire flight control systems. The design procedure combines a methodology for determining sampling requirements, with a direct digital design procedure for control law synthesis, with stochastic estimation as a means for sensor analytic redundancy. Applying the procedure results in facilitating the synthesis step, enhancing control performance, and increasing sensor system reliability and failure tolerance. This paper describes the theoretical basis of the techniques and their application to advanced aircraft designs.

I. Introduction

The application of digital Fly-By-Wire (FBW) technology to the design of aircraft flight control systems has been gaining in popularity. The advantages of digital FBW have been well-documented in terms of improved flight control performance capability, increased capacity to accommodate multiple and complex functions, and increased flexibility to facilitate future modifications. The combination of digital FBW technology with new approaches to aerodynamic design has resulted in Control Configured Vehicle (CCV) designs that are statically unstable, providing considerable advances in aircraft maneuverability, range, and other highly desirable aircraft performance characteristics. This paper advocates the use of modern control theory to aid in the design of digital flight control systems. To date, there has been a reluctance to use modern control theory in the design of aircraft flight control systems due to a lack of practical demonstrations. Recent FBW test bed or technology demonstrator aircraft are providing a means to gain confidence in modern control technology.

Modern control theory offers an organized design procedure to optimally blend multiple controls as well as a means for enhancing system reliability without the proliferation of hardware components. Linear optimal control and stochastic estimation theory are combined to constitute the basis for the recommended design procedure. By using an optimal control technique called discrete implicit model following, we have found that handling quality design specifications may be easily incorporated into the design of the digital controller. Estimation techniques, in the form of a set of reconfigurable steady-state Kalman estimators, can provide sensor analytic redundancy and the necessary optimal control law feedbacks without additional sensor components beyond a conventional flight control sensor set.

This paper outlines our most successful modern control design procedures, highlights the advantages, presents results from sample applications, and establishes generic functional software requirements.

II. Design Principles for CCV Digital Control Systems

An aircraft that is designed using Control Configured Vehicle (CCV) concepts allows the aerodynamic designer to concentrate on performance goals without the classical restrictions of static stability and handling quality performance. Of course, control authority requirements still remain a design parameter which will require airframe and flight control design iterations. In addition, a CCV that is statically unstable imposes a severe reliability and fault-tolerance requirement on the flight control system. As a result, control system synthesis has become a vital part of the aircraft's preliminary design phase and, as shown in Fig. 1, is an integral part of the CCV design cycle. Modern control and estimation theory brings a desperately needed organized design methodology to the CCV design environment. Furthermore, due to rapid advances in computer technology, the application of modern control and estimation theory has become practical as well as providing superior flight control performance.

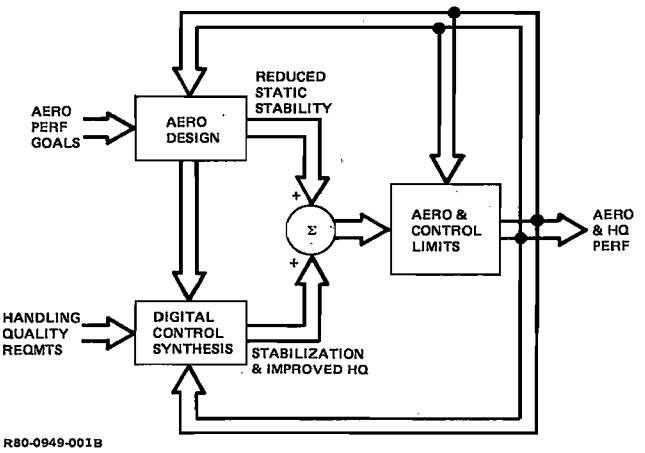

Fig. 1 The CCV Cycle

In this paper, the application of modern control and estimation theory implies the use of linear-quadratic-digital-optimal-control techniques to define feedback flight control laws, and the use of a linear stochastic estimator for state feedback reconstruction and/or analytic redundancy. The synthesis of each will be treated separately (as per the Separation Theorem[1]); however, good estimator design practices will be emphasized to minimize the degradation of robustness or stability margins. The integrated control/estimator system must be verified to ensure compatibility and integrated performance levels. It should be noted that application of optimal control techniques does not imply the need for an estimator, and vice versa.

The following paragraphs summarize the flight control improvements realized through the application of modern control and estimation theory. These are either in the form of facilitating the synthesis step or actual performance improvements.

Improvements Through Optimal Digital Control

As indicated in Fig. 1, proper and robust control is essential to ensure meeting aerodynamic performance goals and handling quality requirements, and stable and safe flying characteristics. A direct digital optimal control approach, such as Discrete Implicit Model Following (DIMF)[2, 3, 4, 5], is a preferred design approach. The advantages of this type of modern control synthesis technique are summarized as follows:

- Application is via computer-aided tools (e.g., Grumman's DIGISYN(6)) which are needed to satisfy the rapid turnaround demands of preliminary CCV design phases

- Direct digital design reduces the design time (e.g., eliminates the need to convert continuous control laws into digital form) and alleviates sampling requirements by no longer penalizing the sampling process with conversion requirements

- Modern control theory offers an organized procedure for optimally blending multiple control effectors to improve mission and handling performance while minimizing crew workload

- Optimal model following techniques offer an organized procedure for introducing handling quality requirements directly into the synthesis step

- Optimal control techniques guarantee robustness(7), or stability margins, resulting in a control loop design insensitive to uncertainties.

Improvements Through Optimal Stochastic Estimation

The applicability of an onboard state estimator is a function of the feedback variables that are needed, their required redundancy, and the ease and accuracy to which these variables can be measured. That is, if providing sensors with sufficient redundancy for all needed measurements is not a problem, and if system noise and aircraft flexibility corrupting the measurements is of little concern, then use of a state estimator is unwarranted. Conversely, flight control system advantages realized through the use of an optimal stochastic estimator is summarized as follows:

- Less sensors are needed to realize a multi-feedback system (e.g., estimates of unmeasured feedback variables are formed using the available measurements)

- When used as a means for analytic redundancy, the state estimator avoids the proliferation of redundant sensors to satisfy failure-tolerance requirements

- Bending compensation can be accomplished through the estimation of aircraft bending states

- Sensor normalization (i.e., removal of bending and kinematic effects) of spatially dispersed redundant sensors can be accomplished using a state estimator

- Estimators can compensate for noise-corrupted and/or bias-corrupted measurements.

III. Digital Control and Estimator Design Procedures

The advantages of direct-digital optimal control and estimator design techniques have been established. As implied, determining the sampling requirements is one of the first steps in the design process. The following paragraphs summarize the design procedures for determining the necessary control loop parameters; namely the sampling requirements, the digital control gains, and the estimator parameters.

Sampling Requirements

An organized procedure for determining sampling requirements is presented in Ref. 8. The procedure determines the minimum sampling frequency for direct digital design control laws. Minimizing sampling frequency is important to avoiding potential computer throughput problems. Although the sample time determination procedure is detailed in Ref. 8, a brief outline is provided here.

The question that is addressed when determining sampling requirements is: "How often must sensor data (e.g., the aircraft states) be examined and the appropriate control reaction applied?" It should be noted that independent functions performed within the flight computer may have different sampling requirements. The primary factors that influence the selection of appropriate sampling frequencies are:

- The desired closed-loop bandwidth in response to pilot inputs

- The allowable aircraft perturbations when the aircraft is exposed to external disturbances

- Fault recovery time requirements.

The latter requirement involves monitoring as opposed to being part of the closed-loop control law computations. That is, based upon monitoring results, decisions are made concerning interruptions and/or reconfiguring normal control operation. How often one must monitor control system operations is independent from how often control-law computations must be executed, and is treated as such. However, the first two items listed above do influence the selection of the required control-law sampling frequency. Experience has shown that a sampling frequency for achieving a desired closed-loop bandwidth will be less constraining than bounding the aircraft's reaction to external disturbances. For example, a 10 Hz sampling frequency would be more than sufficient to satisfy a typical highly responsive closed-loop bandwidth of 2 to 3 Hz.

The rationale for determining sampling requirements based upon allowable perturbations to external disturbances lies in the fact that the aircraft is literally open-loop between sampling instants and will respond completely to these external disturbances. Corrective action to reduce the perturbations is activated at the sampling instants. The maximum allowable sample time is determined by propagating the state covariance matrix and observing the magnitude of the aircraft perturbations as a function of sample time (or the time before corrective action is activated).

Specifically, the stochastic linear matrix differential equation that defines the aircraft dynamics is:

$$\dot{\underline{x}} = A\underline{x} + B\underline{u} + C\underline{w} \qquad (1)$$

where $\underline{x}$ is an n-vector of aircraft states and any augmented noise states; $\underline{u}$ is an r-vector control input, and $\underline{w}$ is an m-vector noise process (which is assumed to be a white process). Propagate the covariance matrix P (i.e., $P = E\{\underline{x}\underline{x}^T\}$) through the numerical solution (e.g., via DIGISYN(6)) of

$$\dot{P} = AP + PA^T + CC^T \qquad (2)$$

where P (o) = 0. After some time T, one or more of the variances (i.e., the diagonal of P) will exceed the boundaries imposed by allowable aircraft perturbations. The elapsed time 'T' is the maximum sample time.

Determination of Digital Control Gains

As previously noted, the digital control synthesis technique(s) that we have found to be most successful in designing aircraft digital flight control laws is Discrete Implicit Model Following (DIMF), which belongs to the control design class of "model in the performance index technique".

The following steps detail the DIMF design procedure.

1. Define the Model. This is perhaps the most difficult step in the entire design procedure because of large differences in opinion as to what time-history characteristics are desirable in

response to a given pilot input. However, once a model response is chosen, a differential equation can be written to describe the desired response. The model will be defined by a matrix differential equation as follows:

$$\dot{\underline{x}}_m = A_m \underline{x}_m + B_m \underline{\delta}_c \tag{3}$$

where $\underline{x}_m$ is the model state and $\underline{\delta}_c$ is the pilot input. The shape of the pilot input is also modeled by a differential equation written as:

$$\dot{\underline{\delta}}_c = A_c \underline{\delta}_c \tag{4}$$

Combining (3) and (4), we obtain a command augmented model given by:

$$\dot{\underline{y}}_m = \begin{bmatrix} \dot{\underline{x}}_m \\ \dot{\underline{\delta}}_c \end{bmatrix} = \begin{bmatrix} A_m & B_m \\ O & A_c \end{bmatrix} \begin{bmatrix} \underline{x}_m \\ \underline{\delta}_c \end{bmatrix} = A_m \underline{y}_m \tag{5}$$

2. Discretize the Model and Aircraft Equations. The discretizing process involves deriving the transition equations, for a given sample period, for both the model and aircraft. For example, if the continuous command augmented aircraft equations are defined as:

$$\dot{\underline{x}}_a = \begin{bmatrix} \dot{\underline{x}} \\ \dot{\underline{\delta}}_c \end{bmatrix} = \begin{bmatrix} A & O \\ O & A_c \end{bmatrix} \begin{bmatrix} \underline{x} \\ \underline{\delta}_c \end{bmatrix} + \begin{bmatrix} B \\ O \end{bmatrix} \underline{u} \tag{6}$$

where $\underline{x}$ is the aircraft state and $\underline{u}$ is comprised of the actuator commands, then the command augmented transition equation for the aircraft is given by:

$$\underline{x}_{a_{k+1}} = \begin{bmatrix} \phi & O \\ O & \phi_c \end{bmatrix} \underline{x}_{a_k} + \begin{bmatrix} F \\ O \end{bmatrix} \underline{u}_k = \phi_a \underline{x}_{a_k} + F_a \underline{u}_k \tag{7}$$

where $\underline{x}_{a_{k+1}}$ and $\underline{x}_{a_k}$ are the command augmented aircraft states one sample period apart. As previously implied, ϕ, ϕ_c, and F are constant matrices that are numerically computed (e.g., via DIGISYN[6]).

The model transition equation using (5) is similarly computed, namely:

$$\underline{y}_{m_{k+1}} = \phi_m \underline{y}_{m_k} \tag{8}$$

where $\underline{y}_{m_{k+1}}$ and $\underline{y}_{m_k}$ are the model states one sample period apart.

3. Define the Performance Index. Our primary objective is to match the aircraft response with the model response. Therefore, we must first relate the aircraft states to the model states; this is accomplished by defining the system output, or measurements, as

$$\underline{y}_k = M \underline{x}_{a_k} \tag{9}$$

where M is chosen so that the dimensions of $\underline{y}_k$ and $\underline{y}_{m_k}$ are the same and that each element of the two state vectors will have similar definitions.

The performance index to be minimized in order to achieve model following is:

$$J_k = \sum_{k=1}^{\infty} (\underline{y}_{k+1} - \underline{y}_{m_{k+1}})^T Q (\underline{y}_{k+1} - \underline{y}_{m_{k+1}}) + \underline{u}_k^T R \underline{u}_k \tag{10}$$

where Q and R are diagonal weighting matrices. Relative Q and R weights are adjusted to either increase or decrease actuator motion. For example, a large R relative to Q will inhibit actuactor motion at the expense of model-following performance.

The above performance index is converted into the standard optimal regulator form by combining (7) through (10) to yield:

$$J_k = \sum_{k=1}^{\infty} \underline{x}_k^T \hat{Q} \underline{x}_k + 2 \underline{x}_k^T \hat{S} \underline{u}_k + \underline{u}_k^T \hat{R} \underline{u}_k \tag{11}$$

where,

$$\hat{Q} = (M\phi_a - \phi_m M)^T Q (M\phi_a - \phi_m M)$$

$$\hat{S} = (M\phi_a - \phi_m M)^T Q M F_a$$

$$\hat{R} = R + F_a^T M^T Q M F_a$$

4. Derivation of the Feedback and Feedforward Gains. The optimal solution of the discrete control problem (i.e., minimization of performance index, 11) results in the surface commands $\underline{u}_K$ being a linear combination of the system states, or

$$\underline{u}_k = K_k \underline{x}_{a_k} \tag{12}$$

where

$$K_k = -(\hat{R} + F_a^T P_k F_a)^{-1} (F_a^T P_k \phi_a + \hat{S})$$

and P_k is the solution of the discrete matrix Ricatti equation

$$P_k = (\phi_a^T P_{k+1} + \hat{Q}) - (F_a^T P_{k+1} \phi_a + \hat{S}) (\hat{R} + F_a^T P_{k+1} F_a)^{-1} (F_a^T P_{k+1} \phi_a + \hat{S}) \tag{13}$$

with $P_\infty = (0)$. It should be noted that the gain elements in K_k associated with the command generator are referred to as feedforward gains, while the remaining elements are the feedback gains.

The Optimal Stochastic Estimator

The advantages of a stochastic estimator has been established. We have had most success[10, 11, 12] with a steady-state Kalman Filter[13]. A functional block diagram of the estimator is shown in Fig. 2. The fundamental estimator equation is given by

$$\hat{\underline{X}}_{k+1} = \underline{X}_k^e + W [Y_{k+1} - M^T \underline{X}_k^e] \tag{14}$$

where

$\hat{\underline{X}}_{k+1}$ is the state estimate at the $(k+1)^{th}$ interval

$\underline{Y}_{k+1}$ is the measurement state at the $(k+1)^{th}$ interval = $M^T \underline{X}_{k+1}$

$\underline{X}_k^e$ is an extrapolation of the previous estimate $\hat{\underline{X}}_k$, given the control command $\underline{u}_k$, so that

$$\underline{X}_k^e = \Phi \hat{\underline{X}}_k + F \underline{u}_k$$

Φ and F are precomputed constant matrices that represent the aircraft transition equations for a given flight condition.

Referring to (14), the state estimate is defined as an extrapolation of the previous estimate that is adjusted by the weighted difference between the measured data and the extrapolated state. The latter difference, known as the estimator residuals, will actively indicate the accuracy of the estimator. Note that the larger the residuals, the larger will be the adjustment to the

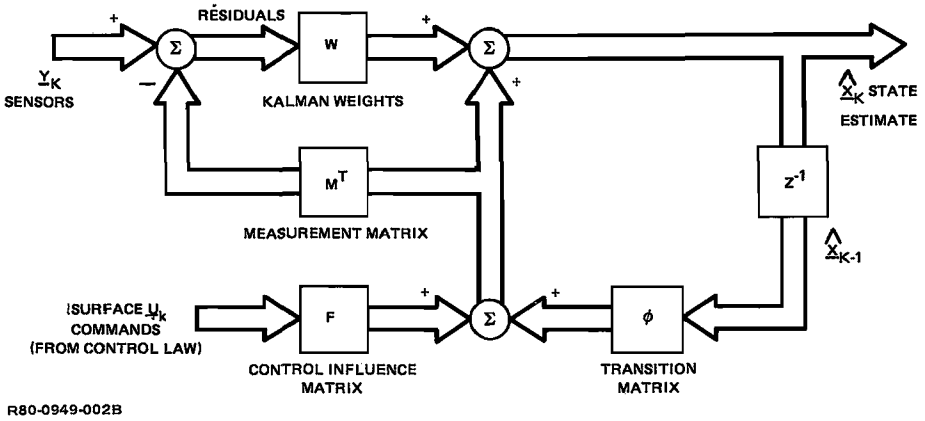

Fig. 2. Estimator Functional Block Diagram

extrapolated estimates. The weights W are discrete Kalman filter steady-state weights that are precalculated to minimize the mean square error between the estimated state and the true state. It can be shown that the z-plane transfer function relating the two input vectors (i.e., $\underline{Y}(z)$, the measurements and $\underline{u}(z)$, the surface commands) to the state estimate, $\hat{\underline{X}}(z)$, is given by:

$$\hat{\underline{X}}(z) = [z\,I + (WM^T - I)\,\Phi]^{-1}\,[zW\underline{Y}(z) + (I - WM^T)\,F\underline{u}(z)]$$
$$= \frac{N_s(z)}{d(z)}\,\underline{Y}(z) + \frac{N_u(z)}{d(z)}\,\underline{u}(z) \qquad (15$$

where

$d(z)$ is a polynominal in z, or the characteristic equation of the estimator whose roots are stable and correspond to the eigenvalues of $(WM^T\text{-}I)\,\phi$

$N_s(z)$ and $N_u(z)$ are matrix polynominals in z, that define the zeroes of the filter.

It should be noted that the implemented steady-state Kalman filter is equivalent, in the classical sense, to a set of parallel, stable, constant-coefficient filters. However, the coefficients are precalculated using Kalman filter theory rather than via classical techniques.

IV. Application of Design Procedures

We have applied the theory described above to several advanced aircraft concepts. The most recent applications included the control law design for Grumman's Forward Swept Wing (FSW) demonstrator[14] and the design of a reconfigurable state estimator as part of a U.S. Air Force funded study entitled "Dispersed and Reconfigurable Digital Flight Control Systems."[12] Some sample results are provided below.

Sampling Requirement Results

As previously noted, the maximum allowable sample time is determined by propagating the open-loop state covariance matrix and observing the aircraft perturbations as a function of time. Figure 3 shows the propagation of the standard deviation of normal acceleration when exposed to clear air turbulence (i.e., using a Dryden spectrum) and an assumed control surface oscillation characterized by a standard deviation equivalent to the least significant bit of a 12-bit digital-to-analog converter. The figure compares normal acceleration oscillations of a present-day fighter with oscillations of the Grumman Forward Swept Wing (FSW) Design. It is noted that FSW normal acceleration oscillations for a given sample time are in general higher than those of the present-day fighter, thus requiring a lower sample time (or faster sampling) for the FSW. Although the FSW is statically unstable subsonically, the increased sampling requirement for this type of aircraft is attributed to improved lifting

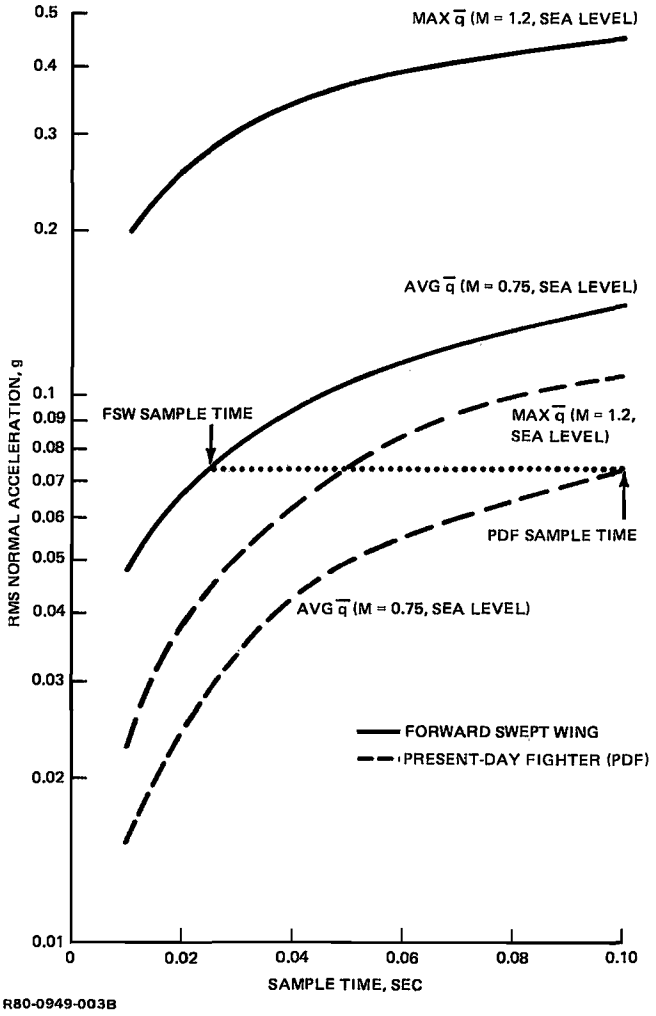

Fig. 3 RMS Normal Acceleration in Clear Air Turbulence Vs Sample Time

efficiency (e.g., FSW C_{L_α} at maximum $\bar{q}$ is three times that of the present-day fighter). The sample times that proved to be acceptable were 0.1 sec and 0.025 sec for the present-day fighter and FSW, respectively. Normal acceleration oscillation levels, at the design sample time, are shown to be identical for the FSW and the present-day fighter at an average dynamic pressure ($\bar{q}$) flight condition. These acceleration levels are considered acceptable for the noted turbulent environment.

Control Law Results

As mentioned previously, the first step in developing model-following control laws is to select a dynamic model to follow. For example, for longitudinal control we have had success by using an ideal short-period respresentation of the dynamics coupled with a first-order stick lag, as shown in Fig. 4. Model constants, such as natural frequency (ω_n) and damping (ζ), are chosen based upon well-accepted short-period handling quality criteria (as per MIL-F-8785B). Other constants, such as the normal load factor coefficient (N_{z_α}) and air speed (V_0), are constrained by the aircraft. The stick lag is introduced as a convenient method for reiterating the design to reduce surface rates. Sample model-following results are shown in Fig. 5.

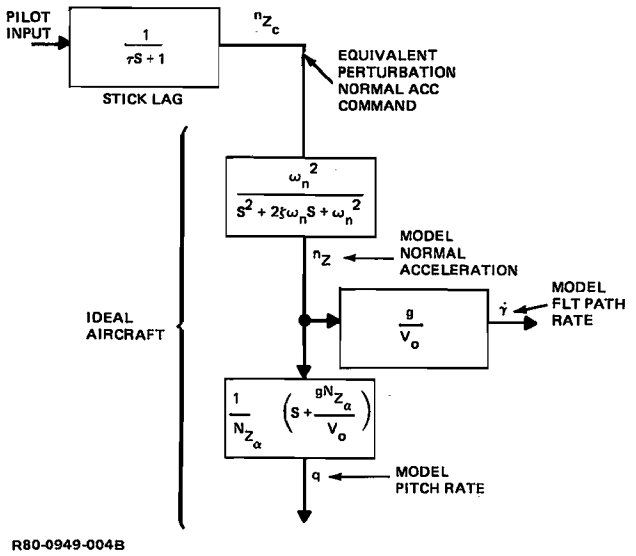

Fig. 4 Desired Longitudinal Dynamic Model

Sets of control gains are determined for several flight conditions through-out the flight envelope. For example, the FSW control system includes 14 gain sets that are scheduled as functions of air data. Linear interpolation is used to avoid gain switching transients. Figure 6 is a functional block diagram of the FSW Up-and-Away Digital Control Laws. The form shown is generic in that the control law consists of control gains multiplying each feedback state and pilot input to produce surface (and possibly throttle) actuator commands. A special feature included in the control diagram is integrated canard control with Automatic Camber Control (ACC). ACC involves collective wing flaperons being driven to minimize trimmed drag. The canard control laws were synthesized by including the ACC logic as part of the aircraft dynamic model. The results, as shown, are crossfeeds from the flap position to the canard command.

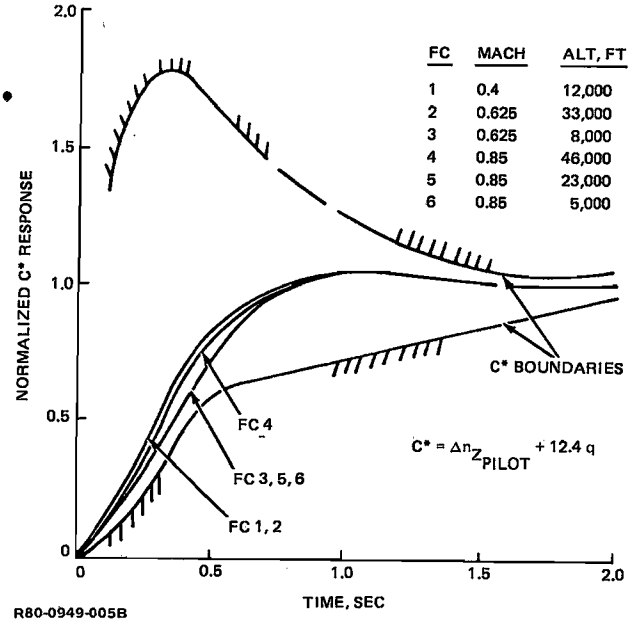

Fig. 5 Model Following C* Step Response for a Present-Day Fighter at Several Flight Conditions

Figure 6 also indicates that the control laws were configured with forward-loop integrators that are executed at twice the fundamental iteration rate. The addition of this form of integral compensation offers the following advantages:

- Reduces the amplitude of the step commands to the actuators or, in other words, provides command smoothing; this also will avoid exciting hydraulic system vibrations
- Increases the "type" of the control loop by one level, which will improve nulling of steady-state errors.

Note that the form of the longitudinal control law shown is a linear combination of past aircraft states as well as present states. The IMF design procedure results in a full-state feedback control law. The unaltered control law form would require feedback of the perturbated integrator output. Since this is an unobservable state (i.e., without knowledge of surface trim), the control law form was transformed into the equivalent form shown. The procedure for transforming the feedbacks, described in Ref 8, is analogous to converting forward-loop integral compensation to feedback integral plus proportional compensation.

The optimal design approach guarantees a 60-degree phase margin. An open-loop frequency analysis verified the phase margins; sample results are shown in Table 1, which includes

FLIGHT CONDITION		PHASE MARGIN, DEG	OPEN-LOOP ZERO GAIN FREQUENCY, RAD/SEC	CRITICAL DELAY TIME, SEC
MACH	ALT, KFT			
0.4	0	58.7	7.4	0.138
0.7	0	70.6	14.2	0.087
0.7	15	59.6	9.4	0.111
0.7	30	58.3	7.7	0.133
1.6	30	73.6	11.6	0.111
0.9	50	60.7	5.8	0.183
1.6	50	66.9	10.6	0.110

R80-0949-011B

TABLE 1 FSW LONGITUDINAL PHASE MARGINS AND CRITICAL TIME DELAYS

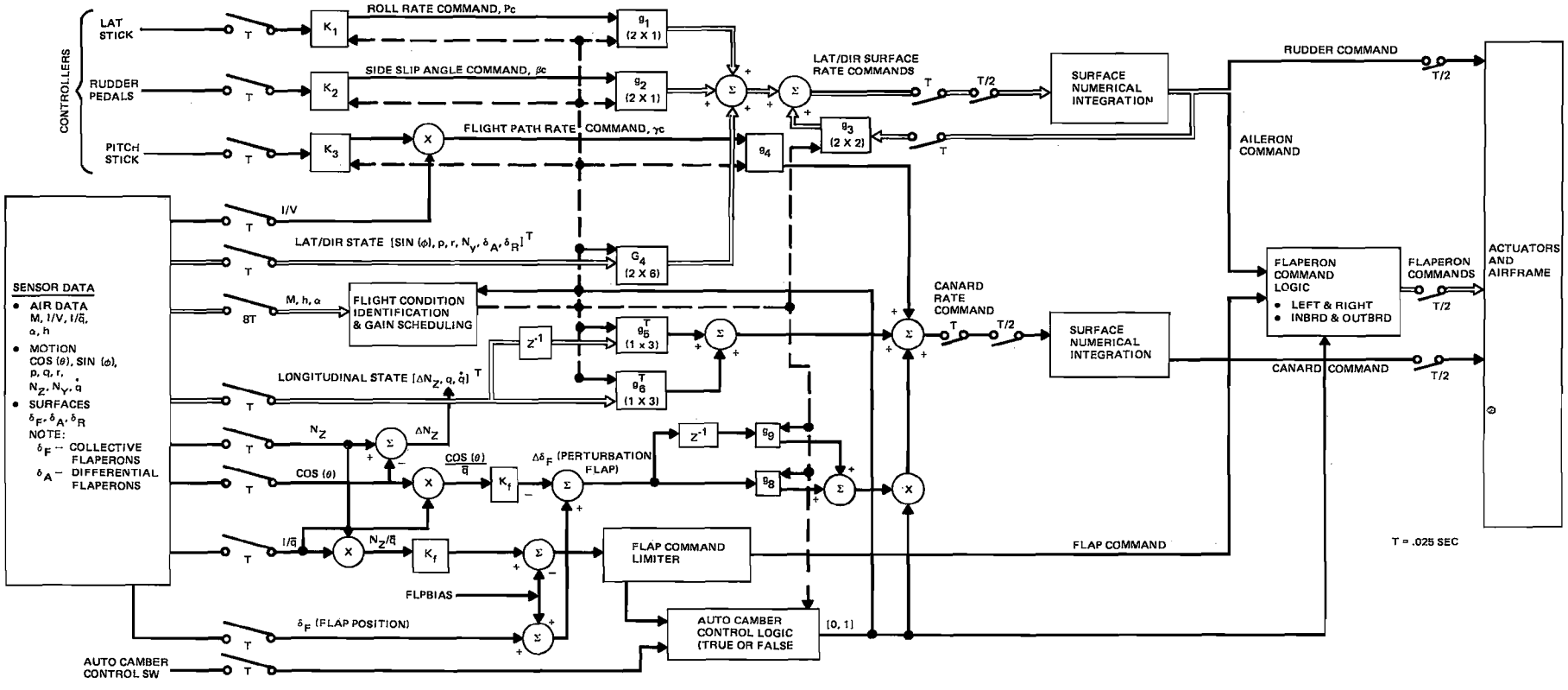

R80-0949-006B

Fig. 6 Three-Axis Digital Control Law Functional Block Diagram for Up-and-Away Flight

the open-loop gain crossover frequency and corresponding tolerable (or critical) time delay. It should be noted that design iterations to achieve reasonable tolerable time delays is a means for desensitizing the closed-loop system.

Estimator Results

During a recent study for the U.S. Air Force[12], a reconfigurable steady-state Kalman estimator was developed for use as a source of analytic redundancy to a baseline set of flight control sensors. Rather than replicating the baseline sensor components to improve the failure tolerance, known analytic relationships between actuator commands and sensed information, and relationships between dissimilar sensor measurements, were mechanized within software as a source of redundant information, ergo, analytic redundancy. These analytic relationships are actually the assumed equations of motion of the aircraft and relationships between the aircraft states and sensor measurements.

The estimator improved the failure tolerance of the baseline sensor set (that was zero to two-failure tolerant) to a sensor system that is three-failure tolerant (3-FOP). The system, which consists of the baseline sensor set, comparison monitoring algorithms (for failure detection and isolation), and reconfigurable estimator, is functionally shown in Fig. 7.

The sensor set that was deemed typical included one inertial navigation system (INS), three lateral and three normal accelerometers, six skewed rate gyros, and two air data systems. Air data systems were included as part of the flight control system sensor set for flight condition identification or gain scheduling. The skewed rate gyros might be considered atypical; however, the system has been fully evaluated (15) and was recently flight-tested. Since the application was for an advanced aircraft with possibly negative static stability, it was assumed that the flight control system was not operational unless all required feedback signals were available. The required aircraft longitudinal motion feedback signals were n_z (normal acceleration at cg), q (pitch rate), and $\dot{q}$ (pitch acceleration); the required lateral/directional feedbacks were ϕ (bank angle), p (roll rate), r (yaw rate), and n_y (lateral acceleration at cg).

Equation (14) established the basic form for each estimator configuration. Aside from providing an analytically redundant source of information, the estimator provides a source for unmeasured control system feedback signals (e.g., $\dot{q}$ — pitch acceleration), plus compensation for noise-corrupted measurements. In order to achieve the goal of three-failure tolerance, a total of 10 estimator configurations were provided. Specifically, there were four longitudinal (1P through 4P) and six lateral/directional configurations (1C through 6C). The estimator was reconfigured as a function of sensor failures, as shown in Table 2. As indicated in Table 2, as long as there are no more than three sensor failures, there is an estimator configuration available to provide signals for all the required feedbacks. For each estimator configuration there was a set of stored constants for each of six flight conditions within the flight envelope. In the event of an air-data failure, constant data were provided for a complete set of 10 estimator configurations. The relationship between the estimator and its interfacing functions are shown pictorally in Fig. 8. Note that the estimator has been separated into two blocks to minimize the processing and, in turn, computation time between sampling the sensor data and updating the actuator commands. The stored estimator coefficients (defined by (14)) were derived for a 10-Hz sampling frequency. It should be noted that all error sources were modeled as uncorrelated white noise for estimator coefficient derivation. In general, unless all error sources are accurately known, it is best to model the errors as uncorrelated white noise in order to desenitize (or improve the robustness of) the estimator to unmodeled errors.

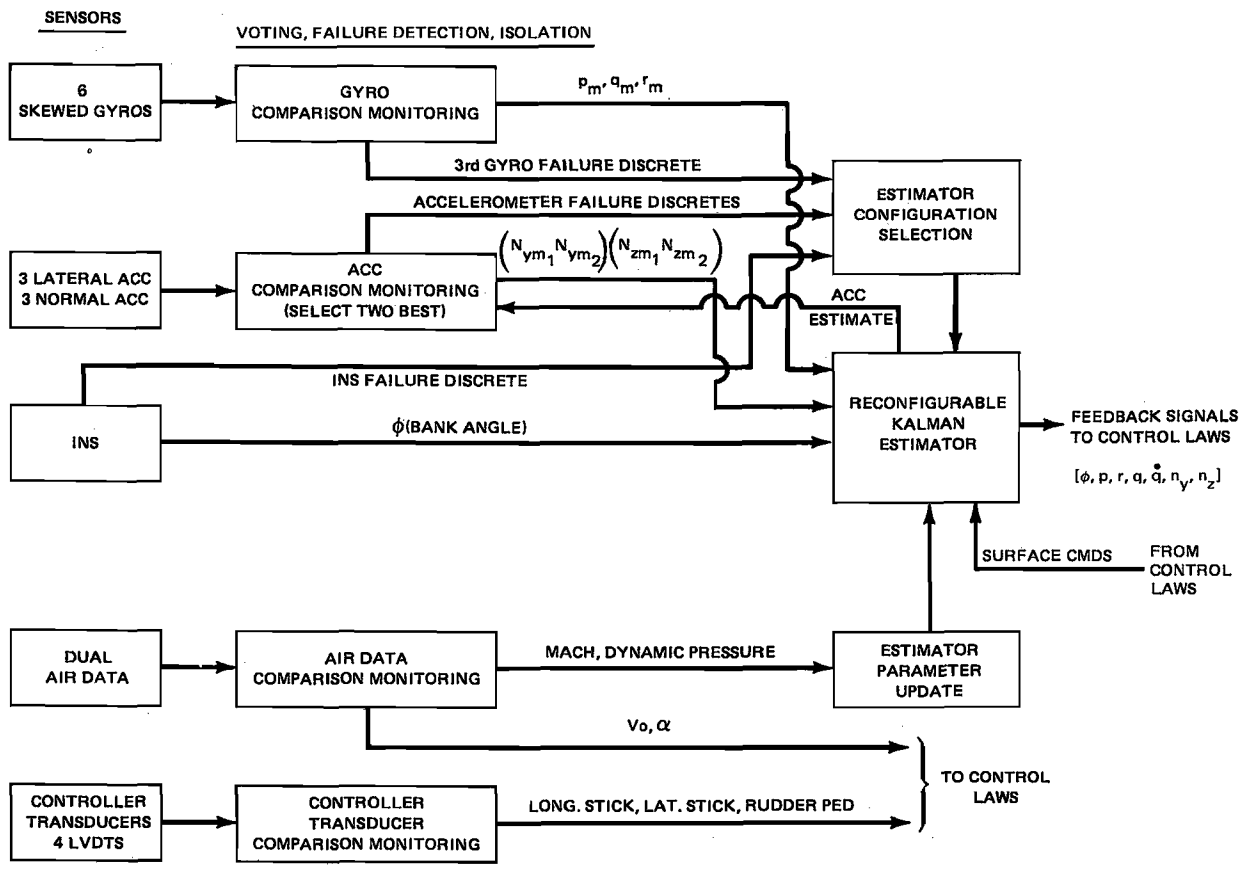

Fig. 7 Integrated Three-Failure-Tolerant Sensor System

LONGITUDINAL SENSOR FAILURES						LONGITUDINAL ESTIMATOR CONFIGURATION			
	NORM ACCELEROMETER			LESS THAN THREE GYRO FAILURES	THREE GYRO FAILURES				
NONE	ONE	TWO	THREE			1p	2p	3p	4p
X						X			
	X			X		X			
		X		X			X		
			X	X				X	
					X				X
	X				X				X

LATERAL/DIRECTIONAL SENSOR FAILURES							LATERAL/DIRECTIONAL ESTIMATOR CONFIGURATION					
		LAT ACCELEROMETERS			LESS THAN THREE GYRO FAILURES	THREE GYRO FAILURES						
NONE	INS	ONE	TWO	THREE			1L	2L	3L	4L	5L	6L
X					X		X					
	X				X						X	
	X	X			X						X	
	X		X		X							X
		X			X		X					
			X		X			X				
				X	X				X			
						X				X		
R80-0949-012B		X				X				X		

TABLE 2 ESTIMATOR CONFIGURATION AS A FUNCTION OF SENSOR FAILURE

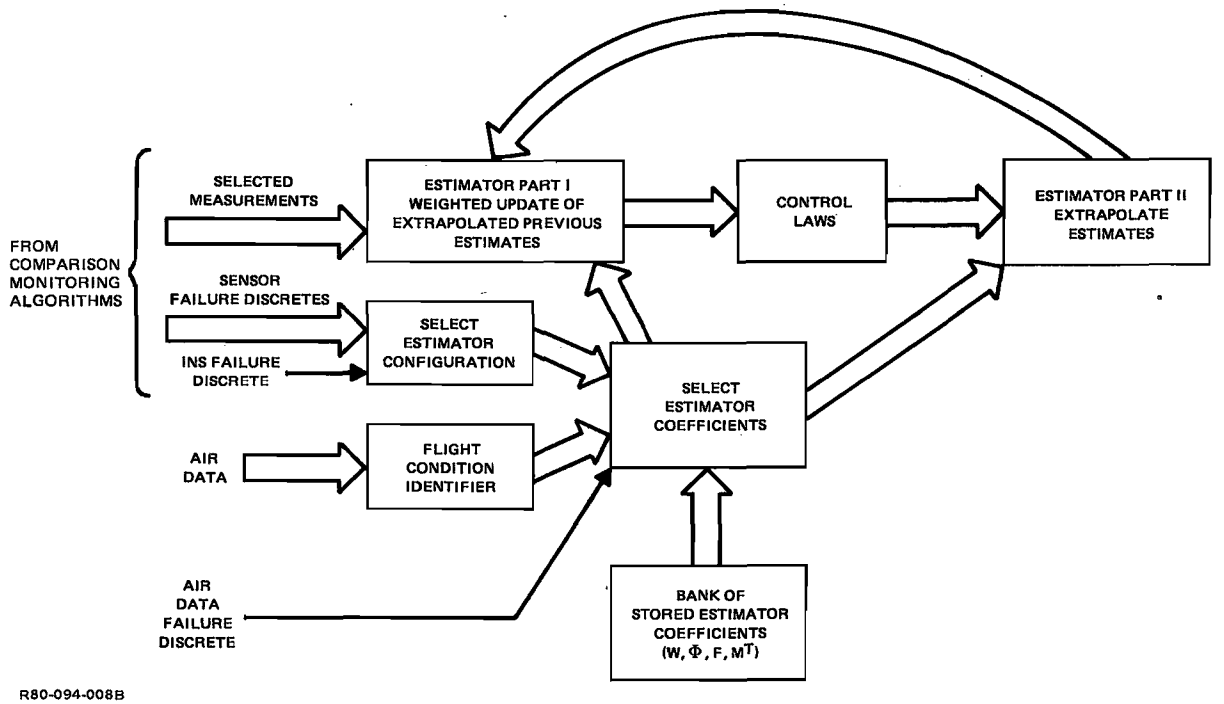

Fig. 8 Reconfigurable Estimator Environment

Given a sensor failure, the estimator is reconfigured by altering the weighting matrix (W in (14)) and forming estimator residuals using the available measurements. Estimator accuracy will decrease as the number of failed sensors increases; this is demonstrated in Table 3.

Analytic redundancy, in the form of a reconfigurable estimator, improves survivability as well as failure tolerance. This is due to dissimilar sensors (e.g., gyros and accelerometers) being dispersed throughout the aircraft. In order to further improve survivability (i.e., to a hostile environment or localized fires), like sensors can be dispersed throughout the aircraft. This was demonstrated in Ref. 12 by dispersing the above noted sensor set to three different locations.

The concern with sensor dispersion within a flexible aircraft is two-fold. First, control interaction with the sensed flexible motion must be avoided. Second, normalization of dispersed redundant sensor signals is required to retain close tracking between like sensor outputs for failure detection and isolation.

FLIGHT CONDITION		ESTIMATOR CONFIGURATION	APPLIED SYSTEM NOISE (1 SIGMA)			ESTIMATION ACCURACY (1 SIGMA)		
MACH	ALT (K FT)		N_z (g)	q (r/s)	$\dot{q}$ (r/s^2)	N_z (g)	q (r/s)	$\dot{q}$ (r/s^2)
0.625	33	1p	0.16	0.014	0.048	0.018	0.0005	0.033
		2p	0.16	0.014	0.048	0.019	0.0005	0.034
		3p	0.16	0.014	0.048	0.02	0.011	0.037
		4p	0.16	0.014	0.048	0.13	0.0005	0.039
0.85	5	1p	0.23	0.010	0.054	0.02	0.0005	0.037
		2p	0.23	0.010	0.054	0.021	0.0005	0.037
		3p	0.23	0.010	0.054	0.022	0.0055	0.042
R80-0949-013B		4p	0.23	0.010	0.054	0.078	0.0005	0.040

TABLE 3 LONGITUDINAL ESTIMATOR ACCURACY

Sensor normalization involves removing bending and kinematic effects from dispersed sensor data. Normalization is accomplished by expanding the previously described estimator. Specifically, the nondispersed estimator equations are augmented to provide estimates of modal rates and accelerations to be used for bending compensation, as well as estimating yaw and roll accelerations to compensate for kinematic effects. The data flow of the dispersed sensor algorithms is shown in Fig. 9. Note that sensor normalization is performed prior to comparison monitoring; i.e., once the normalization process is complete, the algorithms operate as if there is no dispersion.

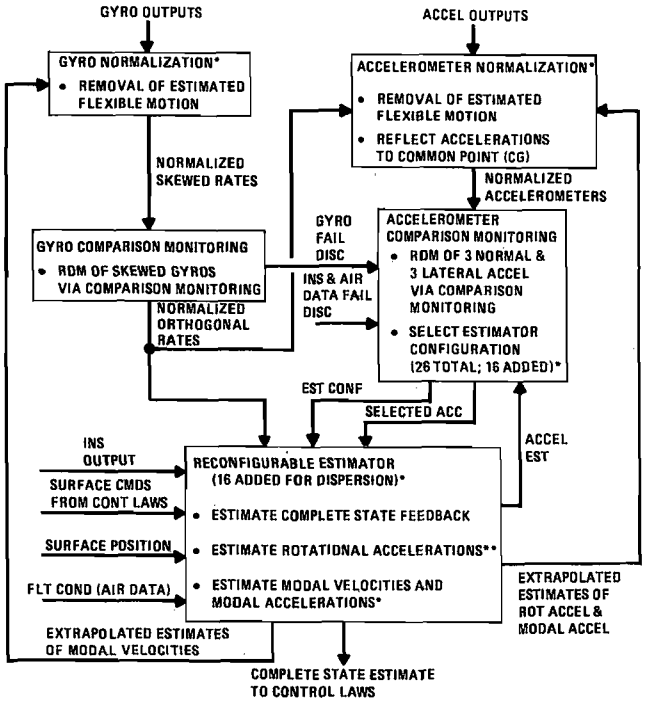

Fig. 9 Dispersed Three-FOP Sensor System Data Flow

Figure 10 shows some simulation results in response to a level turn maneuver. The level turn maneuver is a three-axis maneuver that consists of a 4-sec roll rate command (10 deg/sec) to achieve approximately a 40-deg bank angle, a yaw rate command to help coordinate the turn, and a pitch rate command to maintain level flight. Figure 10A demonstrates the need for sensor normalization. Specifically, without normalization, the figure shows unstable longitudinal control resulting from elevator control interaction with sensed flexible motion. Figure 10B shows results with sensor normalization and with the dispersed 3-FOP sensor system fully operational. Two important observations are made: first, the flexible motion, although excited, is allowed to damp naturally; second, normalization is nearly perfect, as demonstrated by the normalized lateral acceleration measurements as compared to the actual measurements. Figure 10C shows the system's response to three sequential lateral accelerometer bias failures. Table 4 lists time-keyed significant events corresponding to this test run. Note that the control laws were operating without lateral accelerometer measurements at 4.1 sec into the run estimating lateral acceleration via the remaining measurements. All flexible motion was naturally damped without control interaction.

TIME, SEC	SIGNIFICANT EVENT
0	ACC NO. 1 FAILED
0.1	ACC COMPARISON MONITORING TEMPORARILY ELIMINATES ACC NO. 1 THRU VOTING
0.9	ACC NO. 1 ISOLATED AS PERMANENT FAILURE
2.0	ACC NO. 2 FAILED
2.1	ACC COMPARISON MONITORING TEMPORARILY ELIMINATES ACC NO. 2 THRU VOTING; ESTIMATOR CONFIGURATION SWITCHED TO 2-L
3.0	ACC NO. 2 ISOLATED AS PERMANENT FAILURE
4.0	ACC NO. 3 FAILED
4.1	ACC COMPARISON MONITORING TEMPORARILY ELIMINATES ACC NO. 3 THRU VOTING; ESTIMATOR CONFIGURATION SWITCHED TO 3-L
5.1	ACC NO. 3 ISOLATED AS PERMANENT FAILURE
P80-0949-014B	

TABLE 4 SIGNIFICANT EVENTS IN RESPONSE TO THREE SEQUENTIAL LATERAL ACCELEROMETER FAILURES (FIG 10C)

V. Conclusions

Flight control performance and failure tolerance can be enhanced through the application of modern control techniques. Of equal importance is that modern control theory brings an organized methodology to the control configured vehicle design environment to quickly alter designs as preliminary requirements change.

The recommended design procedures included determining sampling requirements based upon allowable aircraft perturbations, formulating feedback control laws using a digital implicit model-following technique, and designing a reconfigurable steady-state Kalman estimator to accomplish the estimation of unmeasured feedbacks, analytic redundancy, and sensor normalization. Hopefully, future technology demonstrator and test bed aircraft will enhance the flight control community's confidence in the advantages and practicality of modern control techniques.

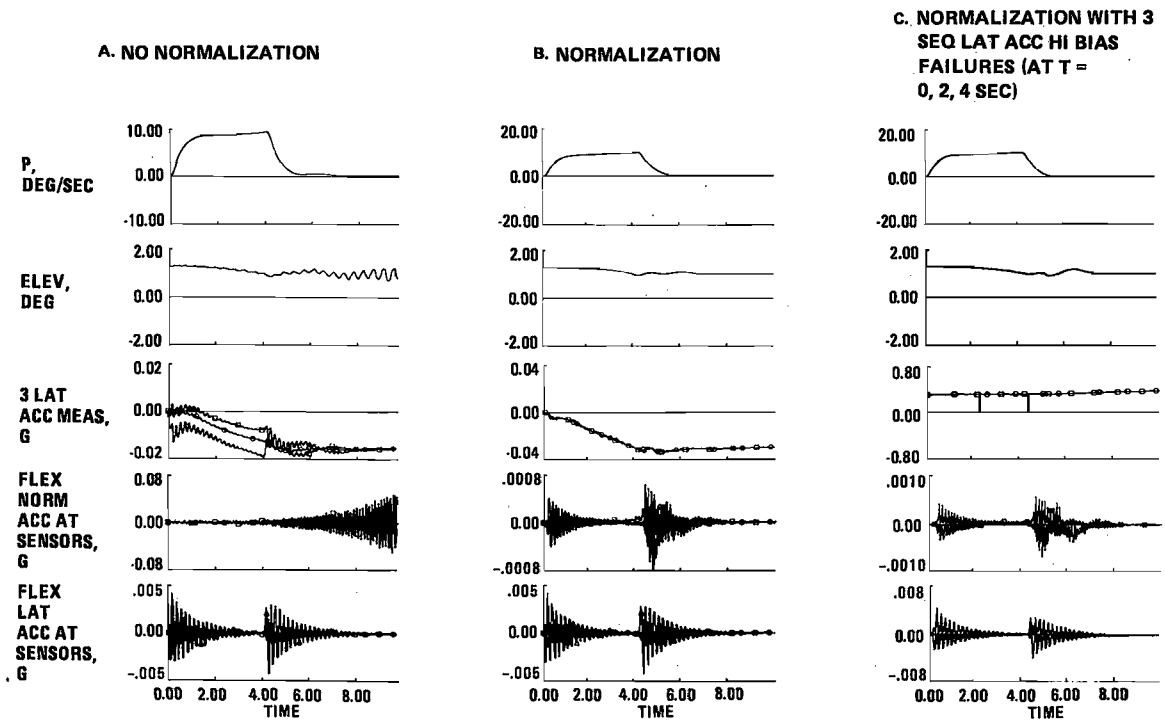

Fig. 10 Level Turn Maneuver at Mach = 0.625, Alt = 33,000 Ft (Present Day Fighter)

VI. References

1. Joseph, P.D. and Tou, J.T., "On Linear Control Theory", AIEE Transactions, Vol. 80, Pt II, Sept. 1961, pp. 193-196.

2. Rothschild, D. and Kreindler, E., "Implicit Model Decoupling Approach to VTOL Flight Control Design," Grumman Aerospace, Bethpage, N.Y., Grumman Research Department Report RE-469, Jan. 1974.

3. Kreindler, E. and Rothschild, D., "New Methods for Command and Stability Augmentation via Optimal Control, Grumman Aerospace, Bethpage, N.Y., Grumman Research Department Report RE-472, April 1974.

4. Morse, A.S., "Structure and Design of Linear Model Following Systems," IEEE Transactions on Automatic Control, Vol. AC-18, Aug. 1973, pp. 364-354.

5. Gran, R., Berman, H., and Rossi, M., "Optimal Digital Flight Control for Advanced Aircraft," Journal of Aircraft, Vol. 14, No. 1, Jan. 1977.

6. Berman, H., "Digital Control Synthesis and Analysis Program (DIGISYN) User's Guide," Grumman Report GCR-77-001, March 1977.

7. Safonov, M. and Athens, M., "Gain and Phase Margin for Multiloop LQG Regulators, "IEEE Transactions on Automatic Control, Vol. AC-22, No. 2, April 1977.

8. Berman, H. and Gran, R., "Design Principles for Digital Autopilot Synthesis," Journal of Aircraft, Vol. 11, July 1974, pp. 414-421.

9. Powell, J. and Katz P., "Sample Rate Selection for Aircraft Digital Control," AIAA Guidance & Control Conference, Aug. 1974.

10. Berman, H., "Digital Control System Synthesis and Laboratory Verification for Fly-By-Wire System Applications," Grumman Aerospace Corp., Report ADR 01-03-76.4, Aug. 1976.

11. Berman, H. and Boudreau, J., "Dispersed Fly-By-Wire Sensor System for Improved Combat survivability," Journal of Guidance and Control, Vol. 2, No. 6, Nov-Dec. 1979.

12. Boudreau, J. and Berman, H., "Dispersed and Reconfigurable Digital Flight Control Systems," AFFDL-TR-79-3125, Vol. 1, Decl 1979.

13. Kalman, R.E., "A New Approach to Linear Filtering and Prediction Problems," Transactions of the ASME Journal of Basic Engineering, Vol. 82D, March 1960, pp. 33-45.

14. "Forward Swept Wing Demonstrator Technology Integration and Evaluation Study," Contract No. F33615-79-C-3036.

15. Weinstein, W., "Development of an Advanced Skewed Sensory Triad (ASSET) System for Flight Control," NADC-76295-30, Oct. 1976.